

Evaluación estructural del tablero compuesto por vigas metálicas del puente sobre el Río Bulubulu, provincia del Guayas

Structural evaluation of the steel girder deck of the bridge over the Bulubulu River, Guayas province

¹ Miguel Angel Intriago Santana



<https://orcid.org/0009-0009-7706-0304>

Faculty of Postgraduate Studies. Technical University of Manabí. Portoviejo, Ecuador.

m-intriago_1311@hotmail.com



² Pablo Julio Lindao Tomala



<https://orcid.org/0009-0002-1144-5518>

Faculty of Mathematical and Physical Sciences. University of Guayaquil. Guayaquil, Ecuador.[pjlinDAO@yahoo.com](mailto:pjlindao@yahoo.com)

Scientific and Technological Research Article

Sent: 05/17/2024

Revised: 06/15/2024

Accepted: 26/07/2024

Published: 08/15/2024

DOI:<https://doi.org/10.33262/conscienciadigital.v7i3.3140>

Please quote:

Intriago Santana, M. Ángel, & Lindao Tomalá, P.J. (2024). Structural evaluation of the deck composed of metal beams of the bridge over the Bulubulu River, Guayas province. ConcienciaDigital, 7(3), 168-192.<https://doi.org/10.33262/conscienciadigital.v7i3.3140>

DIGITAL CONSCIOUSNESS, and It is a multidisciplinary, quarterly journal, which will be published electronically. Its mission is to contribute to the training of competent professionals with a humanistic and critical vision who are capable of presenting their research and scientific results to the same extent that their intervention promotes positive changes in society.<https://conscienciadigital.org>

The journal is published by Editorial Ciencia Digital (a prestigious publisher registered with the Ecuadorian Book Chamber with membership number 663).www.celibro.org.ec

This journal is licensed under a Creative Commons AttributionNonCommercialNoDerivatives 4.0 International License. Copy of the license:<http://creativecommons.org/licenses/by-nc-nd/4.0/>



Palabras

claves:
Evaluación
Puente
Vigas
Metálicas
Diafragmas

Resumen

Introducción: Los puentes son estructuras fundamentales para el desarrollo socioeconómico a nivel mundial, son elementos esenciales para la vialidad y el Ecuador tiene puentes importantes en su red vial. Por otra parte, nuestro país al ser un territorio con un peligro sísmico alto requiere para los puentes no solo un análisis de cargas gravitacionales, si no también bajo cargas laterales provenientes de la acción sísmica. En el presente caso de estudio se abordará el comportamiento estructural del tablero del puente Bulubulu, específicamente comprenderá el análisis a flexión y a cortante de las vigas longitudinales de acero estructural, y el análisis a cargas axiales de los diafragmas de apoyos e interiores. **Objetivo:** Determinar el comportamiento estructural de las vigas longitudinales y diafragmas del tablero del puente Bulubulu antes cargas gravitacionales y carga proveniente de la acción sísmica mediante un análisis modal espectral realizado a un modelo matemático de la estructura elaborado en el programa CSI Bridge. **Metodología:** Revisar los planos estructurales del proyecto original, evaluar las cargas actuantes, elaborar un modelo matemático de la estructura en el programa CSI BRIDGE, realizar un análisis modal espectral al modelo matemático de la estructura, obtener las máximas demandas en las vigas longitudinales y en los diafragmas, verificar las relaciones demanda capacidad (D/C) a flexión y a cortante de las vigas longitudinales, además de las relaciones D/C a compresión y tensión axial de los diafragmas. **Resultados:** De las máximas demandas obtenidas del análisis estructural y de la evaluación de la capacidad de los elementos, se obtuvieron los siguientes resultados. La viga metálica longitudinal “VIGA I (1.360x0.020x0.40x0.03) m tiene la capacidad suficiente para las solicitudes a las cuales será sometida, trabaja al 79% para flexión negativa, 67% para flexión positiva y 25% para cortante. Los diafragmas cumplen satisfactoriamente los requisitos y filosofía de diseño de mantenerse en el rango elástico ante un sismo, para el diafragma de apoyo predomina la compresión en el diagonal trabajando a un 91% de su capacidad, mientras que para el diafragma interior predomina la tensión en el horizontal trabajando a un 49% de su capacidad. **Conclusión:** Mediante el análisis estructural mediante el modelo matemático elaborado en CSI Bridge, se determinaron las máximas solicitudes y más críticas en los elementos de viga longitudinal y diafragmas. Las vigas metálicas longitudinales y diafragmas interiores y de apoyos cumplen satisfactoriamente los

requisitos de diseño bajo la norma AASHTO LRFD 2020, además los diafragmas cumplen con la filosofía de diseño de mantener dichos elementos en el rango elástico. Para este estudio, el diseño de viga longitudinal predomina el Estado Limite de Resistencia I, para los diafragmas de apoyo predomina el E.L Evento Extremo y para los diafragmas interiores predomina el E.L de Resistencia I. **Área de estudio general:** Ingeniería Civil y Mecánica. **Área de estudio específica:** Estructuras Metálicas. **Tipo de artículo:** Original.

Keywords:

Evaluation
Bridge
Beams
Steel
Diaphragms

Abstract

Introduction: Bridges are fundamental structures for socioeconomic development worldwide, they are essential elements for roadways and Ecuador has important bridges in its road network. On the other hand, our country, being a territory with a high seismic hazard, requires for bridges not only an analysis of gravity loads, but also under lateral loads coming from seismic action. This case study will address the structural behavior of the Bulubulu bridge deck, specifically the flexural and shear analysis of the longitudinal structural steel beams, and the axial load analysis of the support and interior diaphragms. **Objective:** To determine the structural behavior of the longitudinal beams and diaphragms of the Bulubulu Bridge deck under gravity loads and seismic loads by means of a spectral modal analysis of a mathematical model of the structure developed in the CSI Bridge program. **Methodology:** Review the structural drawings of the original project, evaluate the acting loads, develop a mathematical model of the structure in the CSI BRIDGE program, perform a spectral modal analysis of the mathematical model of the structure, obtain the maximum demands on the longitudinal beams and diaphragms, verify the demand-capacity ratios (D/C) in bending and shear of the longitudinal beams, as well as the D/C ratios in compression and axial tension of the diaphragms. **Results:** From the maximum demands obtained from the structural analysis and the evaluation of the capacity of the elements, the following results were obtained. The steel beam "VIGA I (1.360x0.020x0.40x0.03) m" has sufficient capacity for the stresses to which it will be subjected, working at 79% for negative bending, 67% for positive bending and 25% for shear. The diaphragms satisfactorily meet the requirements and design philosophy of remaining in the elastic range in the event of an earthquake. For the end diaphragm, compression predominates in the diagonal, working at 91% of its capacity, while for the interior diaphragm, tension

predominates in the horizontal, working at 49% of its capacity. Conclusion: Through structural analysis using the mathematical model developed at CSI Bridge, the maximum and most critical stresses in the longitudinal beam and diaphragm elements were determined. The longitudinal steel girders and the interior and support diaphragms satisfactorily meet the design requirements according to AASHTO LRFD 2020, and the diaphragms comply with the design philosophy of keeping these elements in the elastic range. For this study, the design of the longitudinal beams is governed by Limit State Strength I, the supporting diaphragms are governed by Extreme Event LS and the interior diaphragms are governed by Strength I LS

Introduction

Bridges are fundamental structures for socioeconomic development worldwide. They are essential elements for road traffic and are not exempt from suffering damage and in many cases even collapse due to the forces and loads to which they are subjected during their construction and useful life.

According to Guerra et al. (2021), throughout history the technology with which bridges have been built has evolved since its beginnings more than 3000 years ago when they were manufactured in a rudimentary way with materials such as rock, clay, wood and fibers that served to hold the elements that compose it.

As mentioned Lombeida (2023), nowadays the construction of bridges covers many techniques and it has become necessary to take into account all the constructive factors involved in its process, among the most relevant structural elements are the abutments, the piers, the beams and the deck that depending on the length, as well as the width, the level of traffic, the geological and climatic factors must be designed in order to offer an optimal and safe level of service.

For the design of the BULUBULU bridge, a numerical model was carried out with the SAP 2000 software, considering a beam-type model, with the purpose of capturing the behavior in a more detailed and comprehensive manner (Choi et al., 2019), it is carried out in another software. As mentioned Mañueco (2018), currently, programs such as CSiBridge are used, which is a totally independent software that integrates the modeling, analysis and sizing capabilities of bridge structures in a single model, in addition to considering influence surfaces for vehicular loads (Computer & Structures Inc. [CSI],

www.conscienciadigital.org

2024), and can evaluate lane positioning (National Cooperative Highway Research Program [NCHRP], 2021).

Regarding the present study, the evaluation of the structural behavior of the BULUBULU bridge deck, which is supported on structural steel beams, will be specifically addressed, with the purpose of obtaining a model with a behavior closer to the real behavior of the bridge deck.

Regarding the deck, this constitutes the part of the superstructure of the bridge and is the surface on which the vehicles will circulate and which transmits both loads and overloads to the beams and the rest of the structure. The deck is preferably built in reinforced concrete and sometimes in metal to lighten the dead weight. The deck is also called a slab (Rodríguez, 2020).

Methodology

The methodology used for the present case study will be the quantitative method, which is characterized by the numerical measurement of results. In addition, the type of design is non-experimental descriptive, which is based on observation and does not intend to intervene with the environment. On the other hand, the deductive method will be used, which demonstrates, understands and explains the particular aspects of reality.

The procedure for the case study will be as follows:

- Evaluate the loads that are acting on the bridge in accordance with the AASHTO LRFD 2020 regulations. Such as dead load, vehicular live load, pedestrian live load and seismic action according to the Ecuadorian Construction Standard (NEC, 2015).
- Obtain maximum demands on steel beams and diaphragms.
- Verify the demands versus capacity of the metal elements of the bridge such as longitudinal metal beams and metal diaphragms in accordance with AASHTO LRFD 2020 regulations.
- Check deformations caused by live loads on the Bulubulu Bridge.

Materials and resistances used

For the analysis of the Bulubulu Bridge, the materials considered were concrete and structural steel, which are shown in Table 1.

Table 1

Materials used

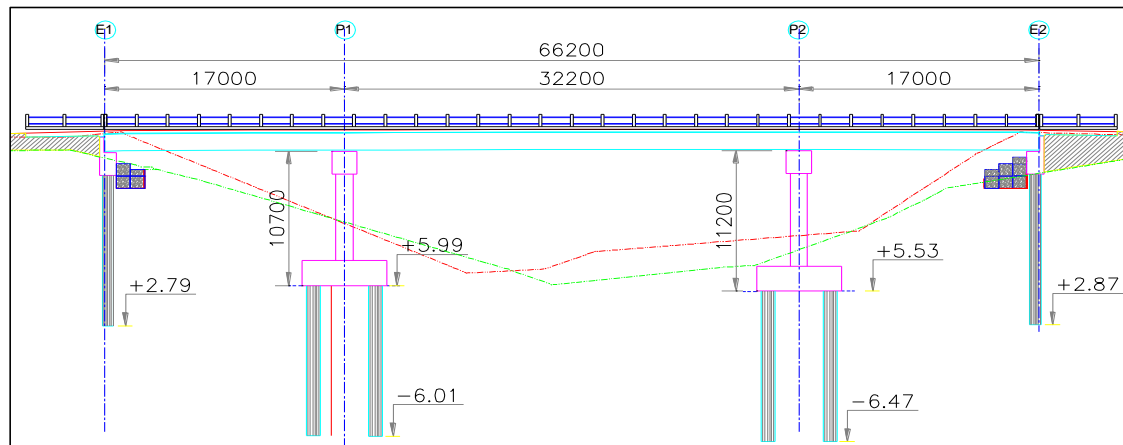
Element	Guy	Specific Weight	Endurance
Slab ts=20cm	5000 psi	2400 kgf/m ³	f _c = 350 kgf/cm ²
Beam	A709Gr50	7850 kgf/m ³	f _y = 3500 kgf/cm ²
Diaphragm	A709Gr50	7850 kgf/m ³	f _y = 3500 kgf/cm ²

Description of the structure

It is located on the Bulubulu River, Km 26 via Puerto Inca - Naranjal belonging to the province of Guayas, Ecuador, it is a beam-type bridge on 2 concrete piles of 10.70m, 11.20m high and on 2 abutments at each end, it consists of 3 spans of 17.00m - 32.20m - 17.00m giving a total bridge length equal to 66.20m (figure 1).

Figure 1

Longitudinal profile of bridge



Analyzed elements that make up the superstructure

The deck is of composite section, has a total width of 10.70 m, which consists of a 0.20 m thick concrete slab, 5 type I metal beams (figure 3). Barrier, pedestrian sidewalk on the left side and Jersey vehicle barrier on the right side. Asphalt layer of 0.075 m thickness, support diaphragms on abutments and piers, intermediate diaphragms in the spans distributed according to figure 2.

Figure 2

Plant, bridge deck

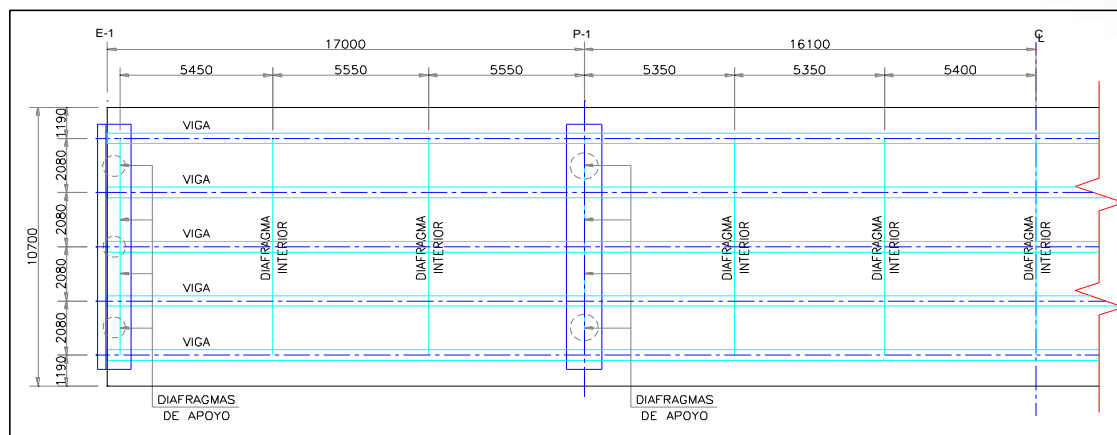
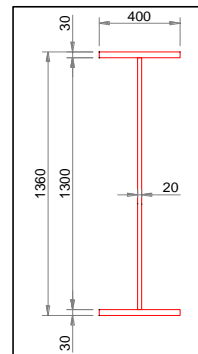


Figure 2 shows a plan view of the deck which is made up of interior diaphragms, support diaphragms and longitudinal metal beams.

Figure 3

Longitudinal Beam "BEAM I (1.36x0.02x0.40x0.03) m"

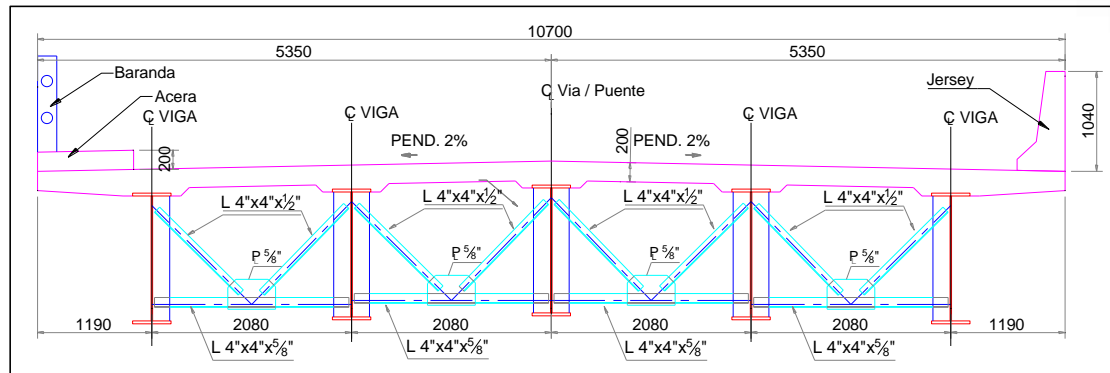


The metal beams are made of I profiles with parallel wings with a yield strength $F_y = 3500 \text{ kg/cm}^2$, these elements are part of the superstructure system (figure 3).

The elements analyzed in this investigation are the longitudinal metal beams, the support diaphragms (figure 4) and interior diaphragms (figure 5).

Figure 4

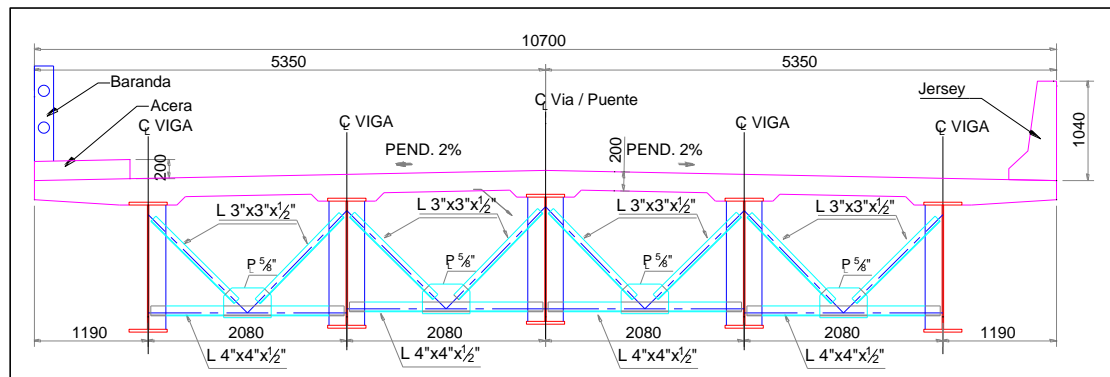
Support diaphragms



The support diaphragms are made of L profiles with a yield strength $F_y=3500 \text{ kg/cm}^2$ with sections of $L4X4X5/8``$ in the horizontal and $L4X4X1/2``$ in the diagonal.

Figure 5

Inner diaphragms



The support diaphragms are made of L profiles with a yield strength $F_y=3500 \text{ kg/cm}^2$ with sections of $L4X4X1/2``$ in the horizontal and $L3X3X1/2``$ in the diagonal (figure 5).

Dead loads

The loads used in the numerical model are those described in Table 2.

Table 2

Dead loads

Element	Thickness (m)	P. Specific (ton/m ³)	Uniform load (ton/m ²)	Guy
Slab	0.2	2.4	0.48	DC

Table 2
Dead loads (continued)

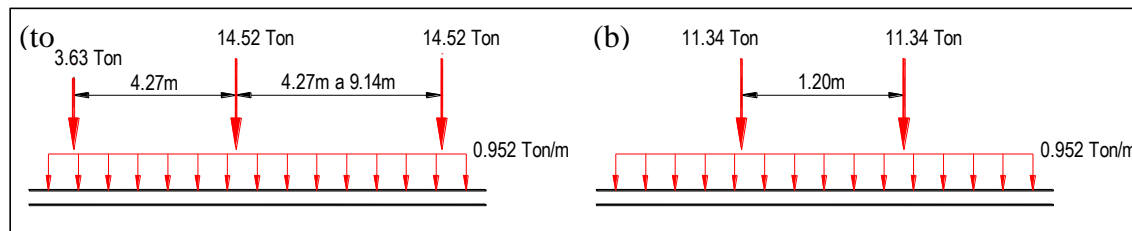
Element	Thickness (m)	P. Specific (ton/m ³)	Uniform load (ton/m ²)	Guy
Sidewalks	0.2	2.4	0.48	DC
Asphalt	0.075	2.2	0.165	DW
Facilities	-	-	0.05	DW
Jersey	A=0.31m ²	2.4	0.74 (ton/m)	DC
Railings	-	-	0.15 (ton/m)	DC

Live loads of vehicles

It is defined according to the American Association of State Highway and Transportation Officials (AASHTO, 2020), art. 3.6.1.2 in which it is designated as HL-93, it consists of a combination of: Design truck or design tandem, and design lane load of 0.952 Ton/m in a width of 3.0m. Multiple presence factor is also considered up to 2 loaded lanes and the increase due to dynamic load.

Figure 6

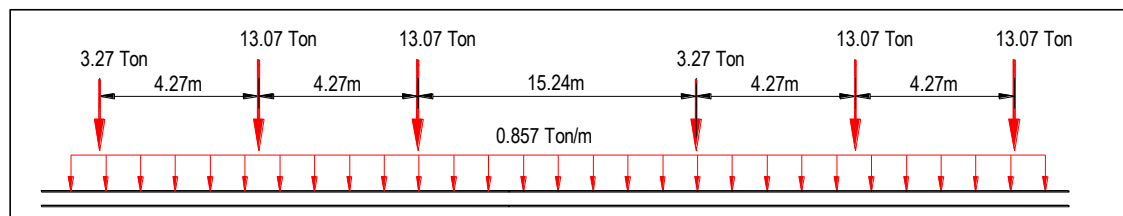
HL-93 vehicle load: (a) design truck + design lane and (b) design tandem + design lane



For negative moment between contraflexure points under uniform load, as well as in the reaction of interior columns, it is defined according to AASHTO (2020), art. 3.6.1.3.

Figure 7

Vehicle setup for negative moment



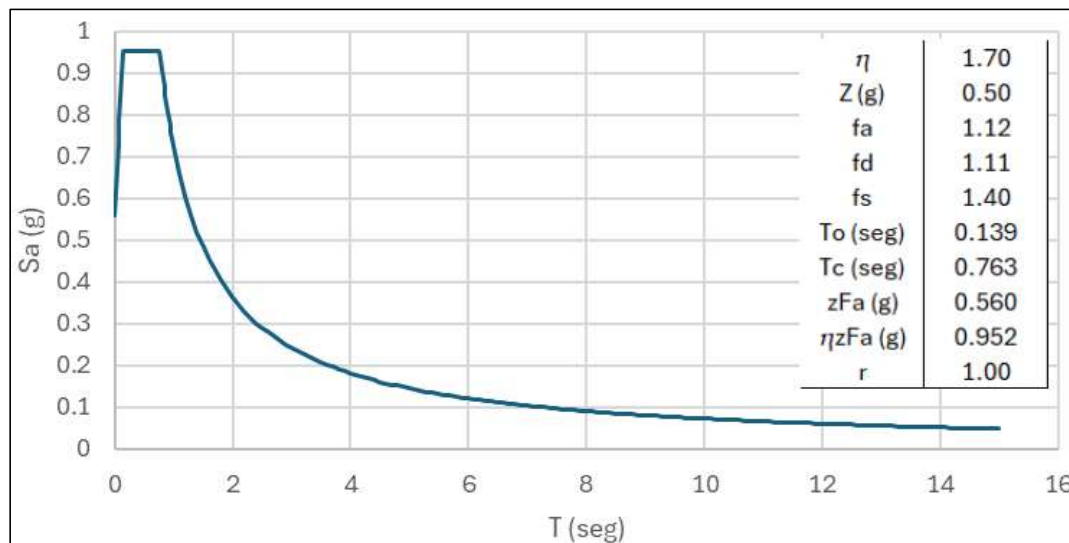
In addition, a pedestrian live load of 0.366 ton/m² on the sidewalk was considered.

Seismic load

The seismic load was defined by means of a design acceleration spectrum defined by the NEC standard (2015), for a design return period $T_r=1000$ years, with a factor $z=0.5g$, type D soil. The response modification factor R , was considered an $R=1$ for the analysis and design of longitudinal beams and intermediate diaphragms (Federal Highway Administration [FHWA], 2014). For the support diaphragms, an $R=2$ was used since a contribution to the dissipation of seismic force by the POT type supports is considered (figure 8).

Figure 8

Design spectrum for Guayas province

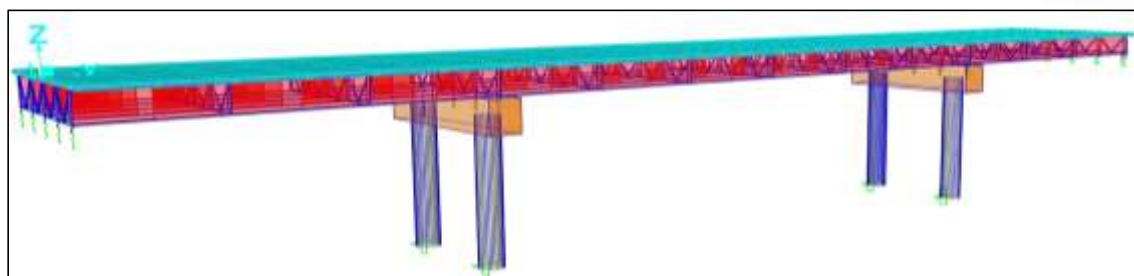


Three-dimensional mathematical model of the Bulubulu Bridge

The mathematical model developed in CSI Bridge will allow obtaining the most realistic behavior of the structure, in which the structural analysis will be performed. The mathematical model is developed in accordance with the geometry and materials described in the previous sections, and embeddings in the abutments and base of columns are considered (Figure 9).

Figure 9

Mathematical model of the Bulubulu Bridge developed at CSI Bridge



Achieving maximum demands

The maximum demands were analyzed for the design combinations according to AASHTO (2020), where the predominant load combinations are:

- Service 1: DC + DW + LL + IM + PL (1)
- Resistance 1: 1.25DC + 1.5DW + 1.75(LL+IM + PL) (2)
- Extreme Event 1: 1.25DC + 1.5DW + 0.5(LL+IM+PL) + EQ (3)

The maximum demands of interest are those placed on the composite beam section (Girder), therefore the following internal force diagrams pertain to the right exterior Girder, which is the critical beam for analysis.

Figure 10

Envelope resistance – DMF (Right Exterior Beam)

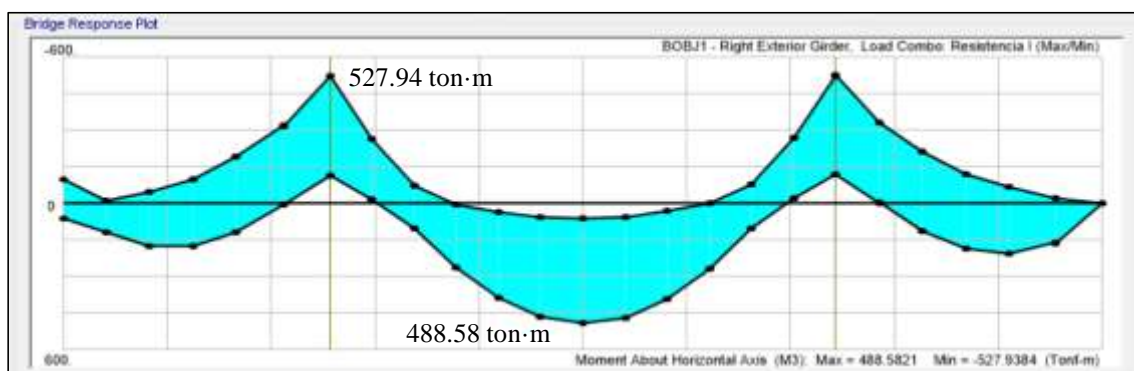


Figure 10 shows the maximum demands obtained per moment in the type I beam by the Resistance envelope I Mu (-) = 527.94 ton m; Mu(+) = 488.58 ton m.

Figure 11

Service Envelope – DMF (Right Exterior Beam)

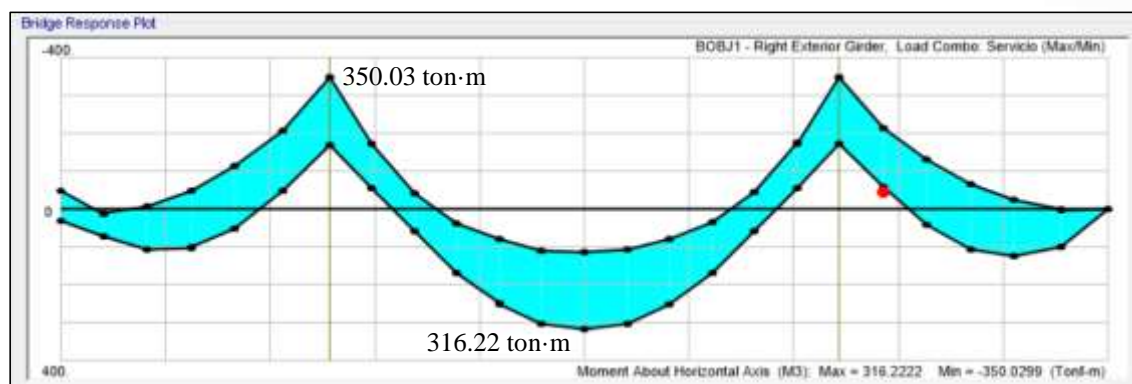


Figure 11 shows the maximum demands obtained per moment in the type I beam by the Service envelope I Mu (-) = 350.03 ton m; Mu(+) = 316.22 ton m.

Figure 12

Surroundextreme event – DMF (Right Exterior Beam)

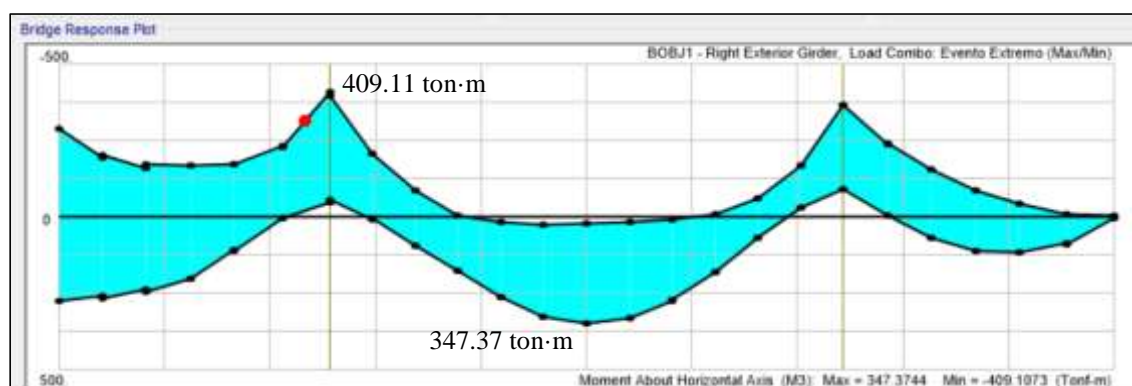


Figure 12 shows the maximum moment demands obtained in the type I beam by the extreme event envelope Mu (-) = 409.11 ton m; Mu (+) = 347.37 ton m.

Figure 13

Envelope resistance – DFC (Right Exterior Beam)

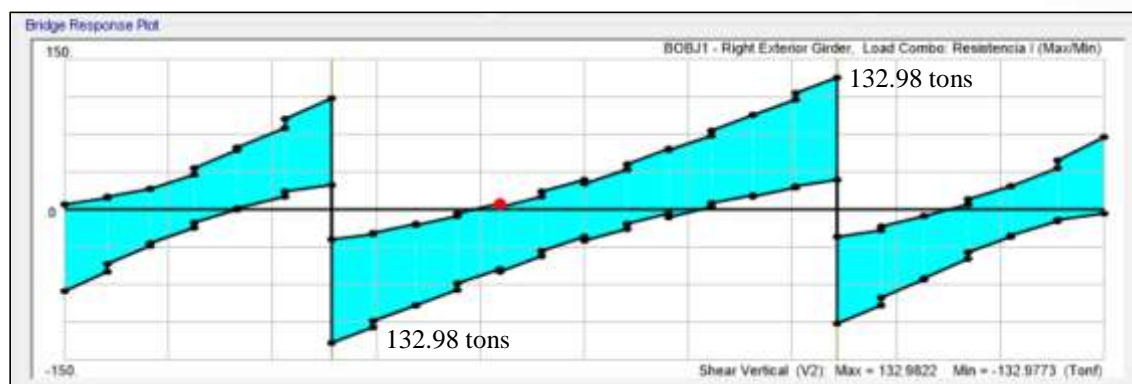


Figure 13 shows the maximum demands obtained by shear force in the type I beam by the Resistance envelope I $V_u = 132.98$ tons.

Figure 14

Service envelope – DFC (Right Exterior Beam)

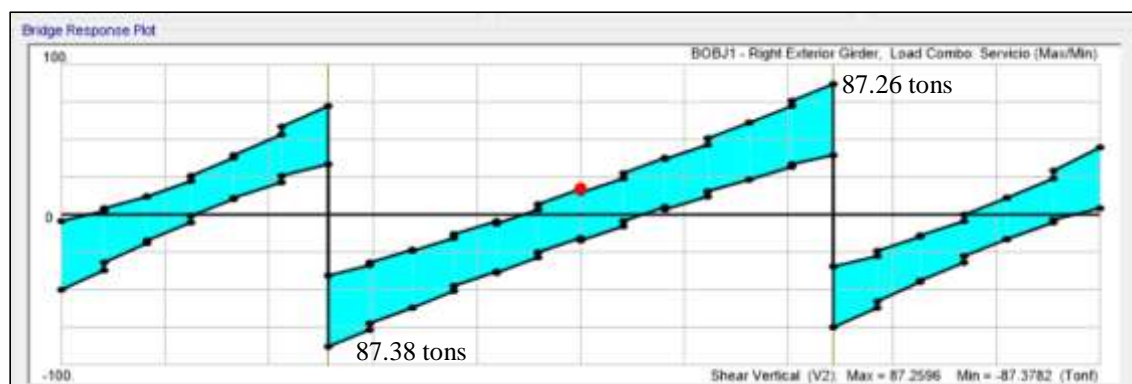


Figure 14 shows the maximum demands obtained by shear force in the type I beam for the Service envelope $V_u = 87.38$ tons.

Figure 15

Extreme Event Envelope – DFC (Right Exterior Beam)

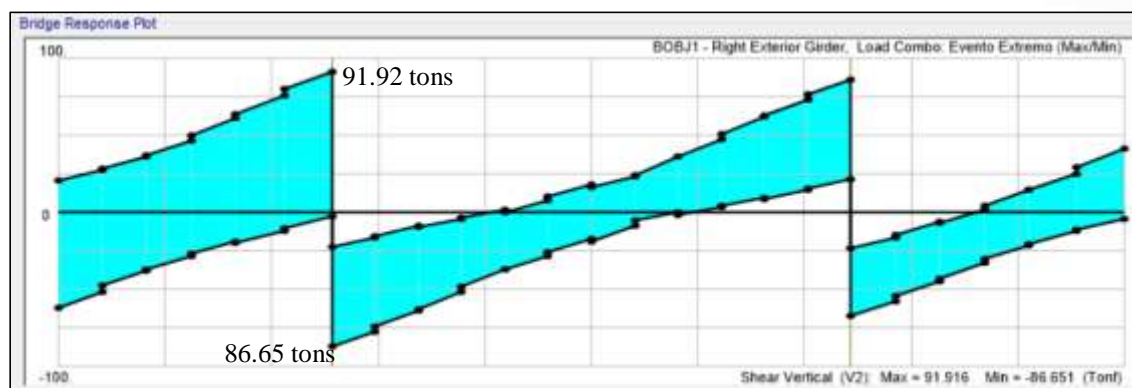


Figure 15 shows the maximum demands obtained by shear force in the type I beam by the Extreme Event envelope $V_u = 91.92$ tons

The maximum demands for the diaphragms were obtained from an envelope that considers Service, Strength and Extreme Event. It can be taken independently without interaction of other efforts (California Department of Transportation [CALTRANS], 2016).

Figure 16

Surround - DFA (Support Diaphragms)

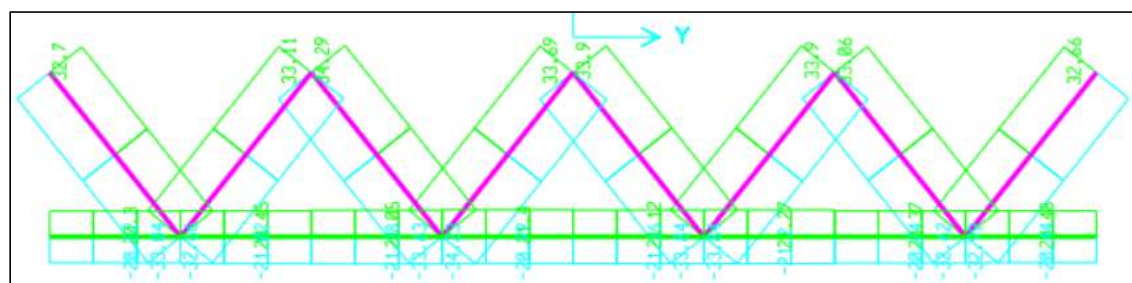
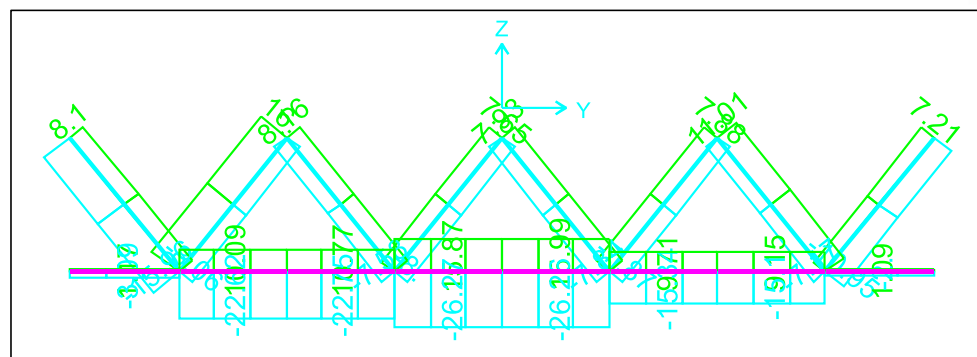


Figure 16 shows the maximum demands obtained by axial load on the support diaphragms by the envelope $F_u (+) = 34.29$ ton; $F_u (-) = 34.23$ ton.

Figure 17

Envelope - DFA (Interior Diaphragms)



Evaluating the envelopes, it is determined that the maximum demands for the beams and diaphragms are those shown in tables 3 and 4 respectively.

Evidently, the Resistance I combination generates greater moment and shear stresses than will control in the resistance limit state (Delgado et al., 2021).

Table 3

Maximum demands on longitudinal beam

Element	Mu + (ton-m)	Mu - (ton-m)	Vu (ton)	Combo
BEAM I (1360x20x400x30)	488.58	527.94	132.98	Resistance 1
Location	x=33.10 m	x=49.20 m	x=49.20 m	

Table 3 shows the location and maximum demands of Bending Moment and Shear Force obtained from the load combinations Service, Strength I and Extreme Event Envelope.

Table 4

Maximum demands on diaphragms

Element	Tension + (ton)	Compression - (ton)	Diaphragm Type	Combo
L4X4X5/8"	21.40	21.38	Support (Horizontal)	Extreme Event
L4X4X1/2"	34.29	34.23	Support (Diagonal)	Extreme Event
L4X4X1/2"	26,26	15.87	Interior (Horizontal)	Endurance
L3X3X1/2"	11.00	7.17	Interior (Diagonal)	Endurance

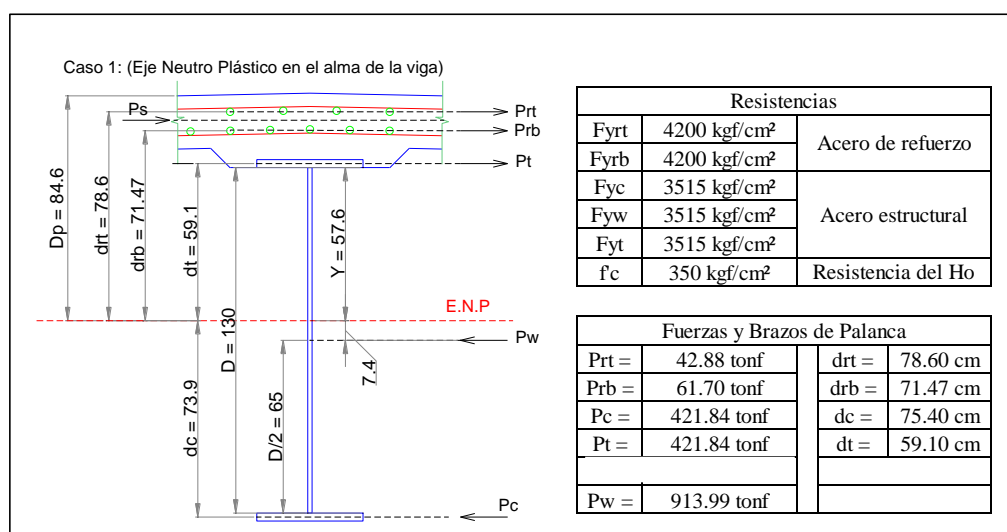
Table 4 shows the maximum axial force demands obtained from the load combinations of Resistance I and extreme event on the diaphragms.

Evaluation of the structural capacity of the elements

Negative bending capacity in beams: The capacity of a composite section beam was evaluated, taking into account the I-beam section plus the contribution of the upper reinforcing steel. First, the plastic neutral axis (PNA) was obtained according to AASHTO (2020), which is located in the beam web, at a distance of 0.576 m measured from the lower face of the upper flange. The equations that apply to the case study are “Case 1” in obtaining the Plastic Moment “Mp” (Figure 18).

Figure 18

Plastic neutral axis (negative bending)



$$M_p = \frac{P_w}{2D} [\bar{Y}^2 + (D - \bar{Y})^2] + [P_{rt}d_{rt} + P_{rb}d_{rb} + P_t d_t + P_c d_c] \quad (4)$$

$$M_p = 946.11 \text{ tonf} \cdot \text{m} \quad (5)$$

The properties of the sections are shown in Table 5.

Table 5

Section Properties

Section	I (mm ⁴)	S bottom (mm ³)	S top (mm ³)
Beam Only	14276866666.7	20995392.2	20995392.2
Composite n=8	30620776710.8	28610465.2	56732972.8
Composite 3n=24	22189821739.9	25520633.7	29965412.8

Table 5 shows the properties of the single beam and composite beam sections, where the Moment of Inertia “I” and Section Modulus “S” are summarized (Chen & Duan, 2014).

Table 6
Yield moment calculation

Moments of Inertia					
Negative moments		Elastic modulus		Yield Moment	
MD1	106.60 tonnes/m	Sncb	0.0209954 m	MAD	1140.07 tonf-m
MD2	50.07 tonf-m	Sstt	0.056733 m	My	1534.36 tonnes-m
MD3	148.75 tonnes/m	Sltt	0.0452379	-	-

MD1=DEAD combination generated moment.

MD2=Moment generated by asphalt.

MD3=Moment generated by DC combination.

My=Yield moment determined as specified in Article D6.2.

$$MAD = Sstt \left(Fyw - \frac{1.25M_{D1}}{S_{ncb}} - \frac{1.50M_{D2} + 1.25M_{D3}}{S_{ltt}} \right) \quad (6)$$

$$My = 1.25M_{D1} + 1.50M_{D2} + 1.25M_{D3} + M_{AD} \quad (7)$$

Table 7 shows how the Beam “BEAM I(1.36x0.02x0.40x0.03) m” works at 79% of its capacity for a negative moment Mu = 527.94 ton-m.

Table 7
Capacity and D/C at negative bending in BEAM

T chamfer	8 cm
Rh	1
Dp	846mm
Dt	1610 mm
Mn	664.34 tonnes-m
Mu	527.94 tonnes-m
φ	1
Mu/φMn	0.79

To determine the capacity, it is calculated based on:

$$Mn = \{Mp \quad \text{for } D_p \leq 0, 1D_t\} \leq 1.3R_hMy \quad (8)$$

$$Mn = \left\{ Mp \left[1,07 - 0,7 \frac{D_p}{D_t} \right] \quad \text{for } > 0,1D_t \right\} \leq 1.3R_hMy \quad (9)$$

Where:

Tchaflan= chamfer+Upper wing

Rh=hybridity factor determined as specified in article 6.10.1.10.1

D_p=Distance between the upper face of the concrete slab and the neutral axis of the composite section when the plastic moment occurs

D_t=Total depth of the composite section (mm)

Positive bending capacity in beams: The neutral axis was calculated for “Case 2” of AASHTO (2020), this is located in the upper flange of the beam, at a distance of 0.025m measured from the bottom face of the upper flange.

Figure 19

Plastic neutral axis (positive bending)

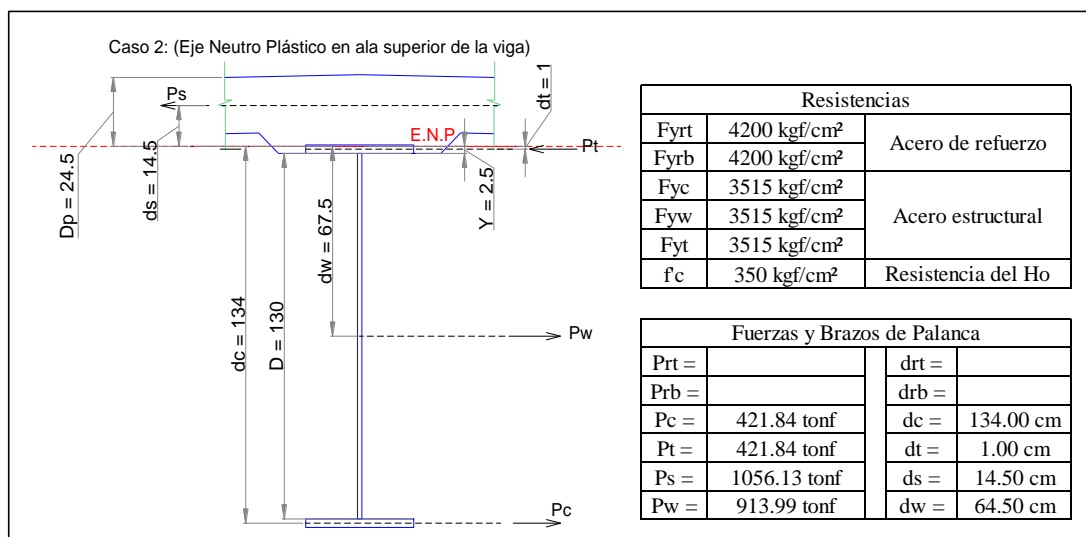


Table 8 shows how the Beam “BEAM I(1.36x0.02x0.40x0.03) mworks at 67% of its capacity for a positive moment Mu = 488.58 ton-m.

Table 8

Capacity and D/C to Positive Bending in BEAM I

Positive Moments		Elastic modulus		Yield Moment	
MD1	84.62 tonf-m	S _{ncb}	0.0209954 m ³	M _{AD}	635.54 tonnes/m
MD2	43.15 tonf-m	S _{stb}	0.0286105 m ³	M _y	942.98 tonnes/m
MD3	109.55 tonnes/m	S _{ltt}	0.0255206 m ³	-	-

Beam Demand/Capacity	
Mn	723.99 tonnes/m ²
Mu	488.58 tof-m
φ	1
Mu/ φMn	0.67

Shear capacity of beams: According to AASHTO (2020), $\phi V_n \geq V_u$ must be fulfilled.

Table 9 shows how the steel beam works at 25% of its capacity for a shear $V_u = 132.98$ tons.

Table 9

Capacity and D/C in shear in BEAM I

Element	Vn	φ	φVn	Vu/φVn
BEAM I (1360x20x40x30) mm	132.98	1	530.115	0.25

$$V_p = 0.58 F_{yw} D_{tw} \quad (10)$$

$$V_n = V_p \left[c + \frac{0.87(1-c)}{\sqrt{1 + \left(\frac{d_0}{D}\right)^2}} \right] \quad (11)$$

Diaphragm compression capacity: According to AASHTO (2020), $\phi P_n \geq P_u$ must be fulfilled.

Table 10

D/C compression on diaphragms

Element	Location	Guy	Pu	φPn	Pu/φPn
L 4"x4"x5/8"	Support	Horizontal	21.38	51.91	0.41
L 4"x4"x1/2"	Support	Diagonal	34.23	37.78	0.91
L 4"x4"x1/2"	Inside	Horizontal	15.87	42.39	0.37
L 3"x3"x1/2"	Inside	Diagonal	7.17	23.27	0.31

Diaphragm tension capacity: According to AASHTO (2020), $\phi T_n \geq T_u$ must be fulfilled.

Table 11

D/C to Diaphragm Voltage

Element	Location	Guy	You	φTn	You/φTn
L 4"x4"x5/8"	Support	Horizontal	21.40	69.61	0.31
L 4"x4"x1/2"	Support	Diagonal	34.29	56.62	0.61
L 4"x4"x1/2"	Inside	Horizontal	26.26	53.35	0.49

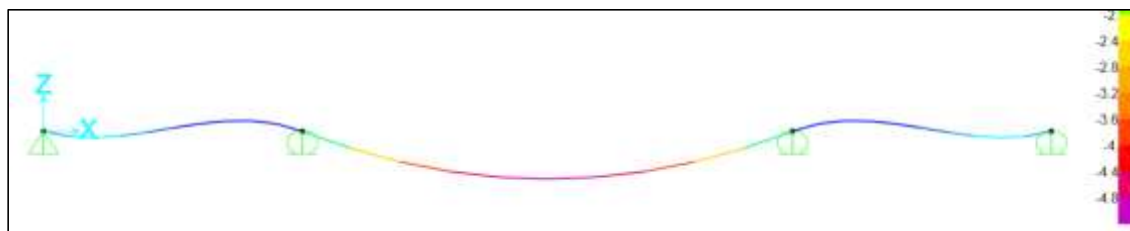
L 3"x3"x1/2"	Inside	Diagonal	11.00	44.76	0.25
--------------	--------	----------	-------	-------	-------------

Deflection analysis

Elastic deflections: Deflections were calculated according to AASHTO (2020), Chap. 3, C2.5.2.6.2 using a structural model of the most critical beam in Sap2000, considering the maximum effect between (case 1: Δ_{truck} or case 2: $0.25\Delta_{truck} + \Delta_{rail}$), it is worth noting that the inertia of the composite beam [short-term properties (η)] were used (Barker & Puckett, 2014). The deformed beam is presented below.

Figure 20

Maximum deflection due to live vehicle load



Considering the allowable deflection as:

$$\Delta_{admissible} = \frac{L}{1000} = \frac{32200 \text{ mm}}{1000} = 32,2 \text{ mm}$$

A deflection distribution factor of: $m g_{deflexion} = \frac{n_{lanes}}{n_{vugas}} = \frac{2}{5} = 0,4$

The maximum deflection is 4.80 mm, case 2 predominates, < 32.20 mm, which is satisfactory.

On the other hand, the Span Length/Superelevation criterion was verified according to AASHTO (2020), Chap. 2, 2.5.2.6.3

Table 12

Verification of Section/Superelevation relationship

Simple Section	Composite Section
$H_{min} = 0.033L$	$H_{min} = 0.033L$
$H_{beam}=$	$H_{girder}=H_{beam}+ts+H_{chamfer}$
$H_{beam} \geq H_{min}, \text{ ok}$	$H_{girder} \geq H_{min}, \text{ ok}$

Permanent deflections: The tension flanges of the composite section were verified for serviceability in accordance with AASHTO (2020), **Chap. 6, 6.10.4.2.**

Table 13 shows how the serviceability is met for Negative Moment in interior and exterior beams, MD1 was considered equal to DC and MD2 as the DW load, while Table 14 shows how it is met for positive moment (American Institute of Steel Construction [AISC], 2022).

Table 13*Serviceability analysis - negative moment*

Interior Beams-Negative Moment						
MD1 (ton-m)	MD2 (ton-m)	MD3 (ton-m)	1.3M LL + IM (ton-m)	S top (beam) (mm3)	S top (girder) (mm3)	Effort (kgf/cm2)
121.21	-	-	-	20995392.16	-	577.32
--	56.23	-	-	-	24892479.29	225.89
-	-	0.00	-	-	24892479.29	0.00
-	-	-	126.86	--	24892479.29	509.63
σ_{total}						1312.84
0.8*Rh*fys						2800
$\sigma_{total} < 0.8*Rh*fys$						OK
Exterior Beams-Negative Moment						
MD1 (ton-m)	MD2 (ton-m)	MD3 (ton-m)	1.3M LL + IM (ton-m)	S top (beam) (mm3)	S top (girder) (mm3)	Effort (kgf/cm2)
148.75	-	-	-	20995392.16	-	708.49
-	50.07	-	-	-	25177234.5	198.87
-	-	0.00	-	-	25177234.5	0.00
-	-	-	157.5	-	25177234.5	625.57
σ_{total}						1532.93
0.8*Rh*fys						2800
$\sigma_{total} < 0.8*Rh*fys$						OK

Table 14*Serviceability analysis - positive moment*

Interior Beams-Positive Moment						
MD1 (ton-m)	MD2 (ton-m)	MD3 (ton-m)	1.3M LL + IM (ton-m)	S top (beam) (mm3)	S top (girder) (mm3)	Effort (kgf/cm2)
103.6	-	-	-	20995392.16	-	493.44
-	43.12	-	-	-	27024466.44	159.56
-	-	0	-	-	27024466.44	0.00
-	-	-	132.56	-	30363621.03	436.58
σ_{total}						1089.58
0.8*Rh*fys						3325
$\sigma_{total} < 0.8*Rh*fys$						OK
Exterior Beams-Positive Moment						
MD1	MD2	MD3	1.3M LL + IM	S top (beam)	S top (girder)	Effort

www.concienciadigital.org

(ton-m)	(ton-m)	(ton-m)	(ton-m)	(mm3)	(mm3)	(kgf/cm2)
109.55	-	-	-	20995392.16	-	521.78
-	43.15	-	-	-	27248089.41	158.36
-	-	0.00	-	-	27248089.41	0.00
-	-	-	168.26	-	30544866.7	550.86
σ_{total}						1231.00
0.8*Rh*fys						3325
$\sigma_{total} < 0.8*Rh*fys$						OK

Conclusions

- Defining the acting loads allowed establishing the most critical condition for gravity loads considering the dead weights and seismic load from an acceleration spectrum according to NEC-SE-DS.
- The structural analysis of the bridge was carried out using a mathematical model in CSI Bridge V.25, which reflected the detailed behavior of the structure under the loads to which it was subjected, thus obtaining the maximum demands for the longitudinal beams and diaphragms.
- The longitudinal beam “VIGA I (1.36x0.02x0.40x0.03) m has adequate bending and shear capacity, working at 79% for negative bending, 67% for positive bending and 25% for shear.
- The diaphragms in supports have good compression and tension capacity, working at 61% tension and 91% compression.
- The horizontal interior diaphragms have good compression and tension capacity, working at 37% in compression and 49% in tension.
- The diagonal interior diaphragms have good compression and tension capacity, working at 31% compression and 25% tension.
- The serviceability verification is satisfactory for “VIGA I (1.36x0.02x0.40x0.03) m, the deflections below L/1000 and stresses lower than those admissible were verified.
- For this study, the longitudinal beam design predominates with EL of Resistance I, for the support diaphragm the Extreme Event predominates, and for the interior diaphragm the EL of Resistance I predominates.

Conflict of interest

The authors declare that there are no conflicts of interest in the submitted manuscript.

Bibliographic References

American Association of State Highway and Transportation Officials [AASHTO]. (2020). LRFD Bridge Design Specifications. <https://store.transportation.org/item/collectiondetail/202>

www.concienciadigital.org

- American Institute of Steel Construction [AISC]. (2022). Steel Bridge Design Handbook. <https://www.aisc.org/nsba/design-and-estimation-resources/steel-bridge-design-handbook/>
- Barker, R., & Puckett, J. (2013). Design of highway bridges an LRFD Approach. John Wiley & Sons, Inc.
<https://onlinelibrary.wiley.com/doi/book/10.1002/9781118411124>
- California Department of Transportation [CALTRANS]. (2016). Seismic design specifications for steel bridges. https://dot.ca.gov/-/media/dot-media/programs/engineering/documents/seismicdesigncriteria-sdc/201605-seismicdesignspecsteelbridges_secondedition.pdf
- Chen, W., & Duan, L. (2014). Superstructure design. Taylor & Francis Group, LLC.
<https://www.routledge.com/Bridge-Engineering-Handbook-Superstructure-Design/Chen-Duan/p/book/9781439852217>
- Choi, B., Moreno, L., Lim, C.S., Nguyen, D., & Lee, T.H. (2019). Seismic performance evaluation of a fully integral concrete bridge with end-restraining abutments. Advances in Civil Engineering, 2019, 12. <https://doi.org/10.1155/2019/6873096>
- Computer & Structures Inc. [CSI]. (2024). CSiBridge bridge analysis, design, and rating. <https://www.csiamerica.com/products/csibridge>.
- Delgado, C., Vera, W., & Rodríguez, R. (2018). Proposal for a bridge applying the AASHTO LRFD design method for the city of Manta. Science Domain, 4(3), 189-210. <https://doi.org/10.23857/dc.v4i3.803>
- Federal Highway Administration [FHWA]. (2014). LRFD Seismic Analysis and design of bridges. US Department of Transportation Federal Highway Administration. <https://www.fhwa.dot.gov/bridge/seismic/nhi130093.pdf>
- Guerra, O., Peña, F., & Yunapanta, J. (2021). Proposal for strengthening solid web beams of metal bridges with carbon fiber and epoxy resin [Master's thesis, Technical University of Ambato, Ambato, Ecuador].
<https://repositorio.uta.edu.ec/jspui/handle/123456789/34195>
- Lombeida, C. (2023). Structural design of a bridge for pedestrian and cattle crossing, in the Pucayacu parish, La Maná canton, Cotopaxi province [Undergraduate thesis, Salesian Polytechnic University, Quito].
<https://dspace.ups.edu.ec/handle/123456789/25260>
- Mañueco, N. (2018). Evaluation of 4 beam-type vehicular bridges over the Rímac River using the MTC inspection manual and csibridge software, Lima 2018

www.concienciadigital.org

[Undergraduate thesis, César Vallejo University, Lima].
<https://repositorio.ucv.edu.pe/handle/20.500.12692/35482>

National Cooperative Highway Research Program [NCHRP]. (2021). Proposed Modification to AASHTO Cross-Frame Analysis and Design.
<https://nap.nationalacademies.org/catalog/26074/proposed-modification-to-aashto-cross-frame-analysis-and-design>

Ecuadorian Construction Standard [NEC]. (2015). Seismic hazard earthquake-resistant design. MIDUVI.<https://www.habitatyvivienda.gob.ec/documentos-normativos-nec-norma-ecuatoriana-de-la-construccion/>

Rodríguez A. (2020). Bridges with AASHTO LRFD 2017 (8th Edition).
https://www.academia.edu/49312415/PUENTES_2020_Ing_Arturo_Rodr%C3%ADguez_Serqui%C3%A9n



www.conscienciadigital.org

The article published is the sole responsibility of the authors and does not necessarily reflect the thinking of the Revista Conciencia Digital.



The article remains the property of the journal and, therefore, its partial and/or total publication in another medium must be authorized by the director of the Conciencia Digital Journal.



Indexaciones

